


RESEARCH

Open Access



Mechanochemical preparation of chrysomycin A self-micelle solid dispersion with improved solubility and enhanced oral bioavailability

Zhuomin Xu¹, Shanshan Zheng¹, Xin Gao¹, Yulu Hong¹, Yue Cai¹, Qiuqin Zhang¹, Jiani Xiang¹, Dehui Xie¹, Fuxing Song², Huawei Zhang¹, Hong Wang¹ and Xuanrong Sun^{1*} 

Abstract

Background: Chrysomycin A (CA) has been reported as numerous excellent biological activities, such as antineoplastic and antibacterial. Though, poor solubility of CA limited its application in medical field. Due to good amphiphilicity and potential anticancer effect of disodium glycyrrhizin (Na_2GA) as an excipient, an amorphous solid dispersion ($\text{Na}_2\text{GA}/\text{CA-BM}$) consisting of CA and Na_2GA was prepared in the present study by mechanochemical technology (roll mill ML-007, zirconium balls, 30 rpm, 2.5 h) to improve the solubility and oral bioavailability of CA. Then, $\text{Na}_2\text{GA}/\text{CA-BM}$ was self-assembled to micelles in water. The interaction of CA and Na_2GA in solid state were investigated by X-ray diffraction studies, polarized light microscopy, and scanning electron microscope. Meanwhile, the properties of the sample solution were analyzed by dynamic light scattering and transmission electron. Furthermore, the oral bioavailability and antitumor ability of $\text{Na}_2\text{GA}/\text{CA-BM}$ in vivo were tested, providing a theoretical basis for future application of CA on cancer therapy.

Results: CA encapsulated by Na_2GA was self-assembled to nano-micelles in water. The average diameter of nano-micelle was 131.6 nm, and zeta potential was -11.7 mV. Three physicochemical detections showed that CA was transformed from crystal into amorphous form after treated with ball milling and the solubility increased by 50 times. $\text{Na}_2\text{GA}/\text{CA-BM}$ showed a significant increase of the bioavailability about two time that of free CA. Compared with free CA, the in-vivo antitumor studies also exhibited that $\text{Na}_2\text{GA}/\text{CA-BM}$ had an excellent inhibition of tumor growth.

Conclusions: $\text{Na}_2\text{GA}/\text{CA-BM}$ nanoparticles (131.6 nm, -11.7 mV) prepared by simple and low-cost mechanochemical technology can improve oral bioavailability and antitumor efficacy of CA in vivo, suggesting a potential formulation for efficient anticancer treatment.

Keywords: Chrysomycin A, Mechanochemistry, Ball milling, Solid dispersion, Self-micelle, Bioavailability, Antitumor

Introduction

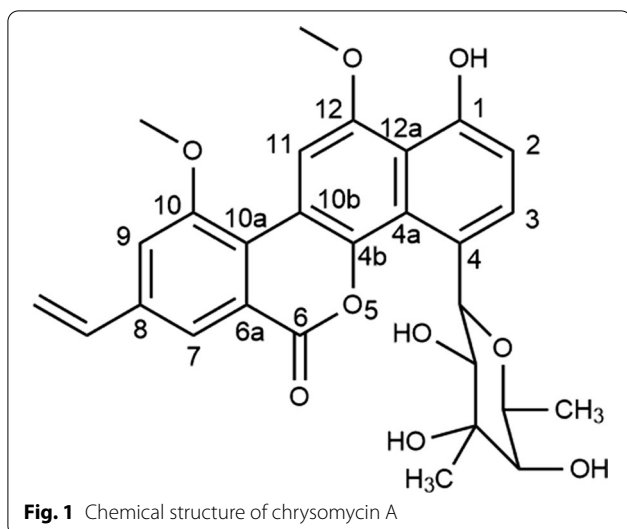
Chrysomycins is a novel antibiotic complex isolated from *Streptomyces* spp, containing compounds of C-glycosides antitumor actives [1]. Especially, Chrysomycin A (CA, Fig. 1) is the major analogue of chrysomycins and plays the most potent role in this complex [2]. Compared with the clinically used anticancer agent doxorubicin,

*Correspondence: sunxr@zjut.edu.cn

¹ Collaborative Innovation Center of Yangtze River Delta Region Green Pharmaceuticals and College of Pharmaceutical Science, Zhejiang University of Technology, Hangzhou 310014, China
Full list of author information is available at the end of the article



© The Author(s) 2021. This article is licensed under a Creative Commons Attribution 4.0 International License, which permits use, sharing, adaptation, distribution and reproduction in any medium or format, as long as you give appropriate credit to the original author(s) and the source, provide a link to the Creative Commons licence, and indicate if changes were made. The images or other third party material in this article are included in the article's Creative Commons licence, unless indicated otherwise in a credit line to the material. If material is not included in the article's Creative Commons licence and your intended use is not permitted by statutory regulation or exceeds the permitted use, you will need to obtain permission directly from the copyright holder. To view a copy of this licence, visit <http://creativecommons.org/licenses/by/4.0/>. The Creative Commons Public Domain Dedication waiver (<http://creativecommons.org/publicdomain/zero/1.0/>) applies to the data made available in this article, unless otherwise stated in a credit line to the data.



CA shows significant cytotoxicity toward cancer cells because of its vinyl group in the 8-position [3, 4]. In addition to strong antineoplastic and antibacterial properties of CA [5–7], it is thought to act as an inhibitor of the catalytic activity of human topoisomerase II [8]. Besides, CA equips with strong antifungal profile, and its cytotoxicity to normal cells can be negligible [2]. Meanwhile, it has no effect on the lysis of red blood cells [6]. All these characteristics indicate that CA has the potential to be a good anti-tumor, anti-bacterial and even anti-fungal candidate. Nonetheless, the oral bioavailability of CA is low owing to its poor solubility in water, which restricts its clinical application. To the best of our knowledge, there are no studies on how to overcome these shortcomings of CA.

Generally, several approaches were employed to improve drug insolubility and bioavailability, such as preparation of polymeric micelles [9, 10], cyclodextrins inclusion complex [11, 12], solid dispersions (SDs) [13, 14], self-emulsifying drug delivery system [15], and so on. In the methods mentioned above, most of them need multiple organic solvents (e.g., dimethyl sulfoxide, *N,N*-dimethylformamide, dichloromethane, etc.), large quantity of surfactants, complex procedures, long preparation time, or expensive excipients (including cholesterol, lipids) [16]. Those are considered unfriendly to the environment, and may increase the risk of solvent exposure during preparation and the cost of production.

Mechanochemical technology has become extensively popular in the field of pharmaceutical sciences for its important role in the development of green synthesis [17, 18], cocrystal synthesis [19, 20], and amorphous SDs [21, 22]. When the high intensity of mechanical energy is transferred to the solid state substances, the strain is generated and may cause plastic deformation and

concurrent changes in the crystal structure along with crystalline phase transitions and amorphization [23]. All the changes may potentially enhance the solubility and bioavailability [24]. Compared with traditional “liquid phase” way, mechanochemical treatment provides significant advantages such as one-step technological process, absence of solvents, and low operating cost.

Disodium glycyrrhizinate (Na_2GA) is the salt formation of glycyrrhizic acid (GA), which can undergo hydrolysis in aqueous solutions and generate free GA. As for GA, it is a good soluble natural saponin, having antiviral [25], anti-inflammatory [26] and anticancer [27] properties. Apart from those features, GA forms non-covalent compounds with various drugs due to its amphiphilicity. Such supramolecular compounds could increase the solubility of hydrophobic drugs up to dozens of times, and enhance the permeability of drug through cell membranes [28–30]. In contrast, Na_2GA solution has lower viscosity and more environment-friendly than GA solution. Meanwhile, Na_2GA has also been reported to have antitumor activity. Zhang et al. [16] formed an amorphous SD of curcumin and Na_2GA utilizing mechanochemistry to enhance the bioavailability and cytotoxic activity of curcumin. Zhu et al. [22] encapsulated SN-38 into Na_2GA for preparing a SN-38 self-micelle SD resulting in markedly improving the solubility and antitumor activity of SN-38.

Given that mechanochemical technology and Na_2GA have the potential to improve the solubility and bioavailability of water insoluble drug, in this study, solid dispersion of CA were prepared mechanical milling with Na_2GA . The physical characteristics, solubility, pharmacokinetics, tissue distribution and anti-tumor activity of CA as an amorphous SD were further investigated.

Materials and methods

Materials

CA was obtained from professor Fuxing Song (Beijing Technology and Business University, purity >99%). Disodium salt of glycyrrhizic acid (Na_2GA) was purchased from Shanxi Pioneer Biotech Co. Ltd. (Xian, China, purity >98%). Acetonitrile was obtained from Tedia Company, Inc. (Fairfield, OH, USA, HPLC grade). Formic acid with purity >88% was purchased from Aladdin Bio-Chem Technology Co., Ltd. (Shanghai, China). Roswell Park Memorial Institute 1640 (RPMI-1640) cell culture medium, fetal bovine serum (FBS) and penicillin/ streptomycin were all purchased from Gibco BRL (Gaithersburg, MD, USA).

Cells and animals

The mouse melanoma cell line B16-F10, the human breast cancer cell line MCF-7, the human hepatocellular carcinoma cell line HepG₂ was purchased from the China

Center for Type Culture Collection (Wuhan, China). The cells were cultured in RPMI-1640 (B16-F10 cells) or DMEM (MCF-7 cells and HepG2 cells) containing 10% FBS and 1% antibiotics (penicillin/streptomycin).

Female ICR mice (5–6 weeks of age, 18–20 g body weight) and female C57BL/6 mice (5–6 weeks of age, 16–18 g) used in the experiments were provided by the Zhejiang Academy of medical Science, conducting with the approval of the animal experiment center of Zhejiang University of Technology. All the animals were performed in strict compliance with the PR China legislation for the use and care of laboratory animals.

Fabrication of nanoparticles by mechanochemical treatment

The roll mill ML-007 (Wiggins, German) was used to prepare samples. Briefly, 0.15 g CA and 14.85 g Na₂GA (weight ratio 1/99) were added to 300 mL vial with 660.0 g zirconium balls (diameter 22 mm) with milling time of 3 h, rotation speed 30 rpm and samples were picked out at 0.5, 1, 1.5, 2, 2.5 h, and 3 h, respectively. In addition, a mixture of Na₂GA and CA (weight ratio was same as above) by ordinary physical treating without ball milling, were prepared for comparing with the ball milling products. At last, the ball-milling products with different milling time were described as BM-0.5 h, BM-1.0 h, BM-1.5 h, BM-2.0 h, BM-2.5 h, BM-3 h, and the physical milling product was described as Na₂GA/CA-PM.

Analysis of chrysomycin A by HPLC

The appropriate amounts of samples were dissolved completely in a mixture solution (deionized water to acetonitrile, 1:1, v/v) respectively, and filtered through a 0.22 μm filter paper. Then, the filtrate was determined by a high performance liquid chromatography (HPLC, Agilent 1260 infinity II) equipped with column Inertisil O DS-3 C₁₈ (250 mm × 4.6 mm, 5 μm, GL Science Inc., Japan) at 25 °C, and a UV detector set at a wavelength of 254 nm. Acetonitrile—0.1% formate water (40:60) was used as eluent (pH = 2.6–2.8) with the flow rate of 1.0 mL/min.

Solubility determination

To determine the solubility, an overdose of samples and CA, were put into 500 μL of deionized water respectively and stirred for 12 h at 25 °C. Finally, these solutions were filtered and analyzed by HPLC.

Powder X-ray diffraction (XRD)

X-ray diffraction test of samples was implemented with a Bruker D₂ Phase diffractometer (Baker, Germany) by using CuKα radiation. Step range: 3°–40°. Counter speed:

3.7°/min. All the data were analyzed through GraphPad Prism 7.

Polarized light microscopy (PLM)

To distinguish the refraction phenomenon of samples, a small amount of solid powder was placed on microscope slide and observed by an Olympus CX41 polarized microscope (Japan) with a CCD camera (HTC1600, China). All the pictures were obtained at 10× resolution.

Scanning electron microscopy (SEM)

After samples were coated with platinum by a Leica EM ACE200 Vacuum Coater (Germany), SEM (ZEISS Gemini500, Germany) was performed to acquire electronic images. The Coating parameter: amperage 30 mA, spraying time 100 s.

Particle characterization, zeta potential and stability

The physicochemical properties of samples containing hydrodynamic diameter, polydispersity index (PDI), and zeta potential, were detected using dynamic light scattering (DLS) instrument (Zetasizer NanoZS, Malvern Instruments, Malvern, UK) at 25 °C. Before being measured, all samples were dissolved in deionized water at the concentration of 1 mg/mL, then filtered by a 0.22 μm filter. The sample was dissolved in DMEM with 10% FBS. Then the change in particle size and PDI of micelles were measured for 72 h.

Determination of the critical micelle concentration

3 μg of Nile red dissolved in 90 μL CH₂Cl₂ was added to a series of vials, and CH₂Cl₂ was evaporated at room temperature. The aqueous solutions of ball milling sample with various concentrations ranging from 0.001 to 10 mg/mL were added into the vials, stirred for 12 h. The fluorescence intensity of Nile red (excitation wavelength: 579 nm, emission wavelength: 620 nm) in these solutions was measured by a microplate reader (Flexstation 3, Molecular Devices LLC, Sunnyvale, CA, USA).

Transmission electron microscopy (TEM)

To observe the morphology of micelle, samples were configured into 1 mg/ml solution. One drop of sample was dripped on a carbon Formvar-coated copper grid for a minute, and then were dried below the infrared light. Finally, TEM (Hitachi HT700 EXALENS, Japan) was at a working voltage of 100 kV to form the morphology of samples.

In vitro cell viability studies

Cell viability of free CA, Na₂GA, and the ball milling sample on MCF-7, HepG₂, and B16-F10 cells was evaluated by MTT assay. The cells were incubated in 96-well

plates at a density of 4×10^3 cells per well. After 12 h of incubation at 37 °C with 5% CO₂, the medium was replaced by 100 µL fresh medium containing the suspension of free CA, Na₂GA, or the ball milling sample with a series of concentration. After another 48 h of incubation, the medium was removed and the fresh medium containing 10 µL of MTT (5 mg/mL) were added to each well. The cells were further incubated for 4 h, then the medium was removed, and 100 µL DMSO was added to dissolve the formazan crystals. The absorbance of each wells was measured by a microplate reader at the wavelength of 570 nm. Cell viability in each group was expressed as a percentage relative to that of the untreated control.

Cellular uptake studies

For qualitative analysis and intracellular localization, coumarin-6-loaded ball milling products (NPs/C6) were prepared. 1 mg coumarin-6, were mixed with 1 mg Na₂GA/CA-BM powders and then dissolved in 200 µL tetrahydrofuran completely. Then about 1 mL distilled water was added dropwise with continuously stirring for extra 12 h. When tetrahydrofuran was evaporated, the labeled NPs were stored at - 20 °C.

B16-F10 cells were seeded in a 24-well plate as a density of 2×10^4 cells per well, and incubated for 12 h before use. Then the cells were incubated with 10 µg/mL NPs/C6. Four hours later, the cells were washed three times with 4 °C PBS, fixed with 4% paraformaldehyde for 15 min at room temperature, and stained with Hoechst33342 for another 10 min. Finally, the plate was observed under a fluorescence microscope (Olympus IX73, Japan) after washed with 4 °C PBS three times.

Pharmacokinetic evaluation

Ten female ICR mice were randomly divided into two groups (CA and the ball-milling product) to evaluate the pharmacokinetic of samples. The samples were dispersed in deionized water and were intragastrically administered to the mice at the equivalent dose of 50 mg/kg CA. Next, 0.2 mL of blood was collected into prepared heparinized tubes at different time points (0.25, 0.5, 1, 2, 4, 8, 12, and 24 h) after administration, and then centrifuged at 5000 rpm, 4 °C for 5 min to obtain plasma supernatant. After taking plasma to a cleaning tube, a certain volume of acetonitrile was added to the supernatant (the volume ratio was 3:1). When protein precipitates generated, the mixture was vortexed for 2 min, and centrifuged at 10,000 rpm, 4 °C for 10 min. Then, supernatant from the mixture was extracted and stored at - 80 °C for 2 h for further use. After being thawed, samples were centrifuged (10,000 rpm, 4 °C) for 10 min and take out. At last, the sample was filtered by a 0.22 µm filter for HPLC analysis.

In vivo tissue biodistribution study

To investigate the tissue biodistribution of CA and the ball-milling product, ten female ICR mice were stochastically divided into two groups. The ball-milling sample and CA were formulated as suspensions at a concentration of 5 mg/mL. The dose for each intragastric administration was 50 mg/kg equivalent to the concentration of CA. At the set time points (2 h, 6 h, 12 h), major organs containing heart, liver, spleen, lung, kidney, brain, skeletal muscle were resected and wash with 10 mM phosphate buffered saline (PBS). After being dried and weighted, the organs were divided into small pieces and homogenized with deionized water at ratio of 1:2 (g/mL). To extract CA from tissues, the homogenate was added with acetonitrile (the ratio was 1:3). Then the mixture was vortexed for 1 min and centrifuged at 10,000 rpm, 4 °C for 10 min. Ultimately, supernatant was removed from the mixture to a clean tube and stored at - 80 °C for HPLC analysis.

In vivo antitumor efficacy

The tumor-bearing model was established by subcutaneously injecting 1×10^6 B16-F10 cells in 100 µL of PBS into female C57BL/6 mice at the right flank. When the tumor volume reached to about 35–60 mm³, the mice were casually divided into three groups (n=6/group). Each mouse was intragastrically administered with an equivalent dose of 50 mg/kg CA (Na₂GA/CA-BM and CA suspension) every 2–3 days, whereas the control group was given PBS. The volume of administration was 200 µL per mouse.

The first day of administration was recorded as day 0, the tumor growth and body weight change were monitored every 2–3 days. The tumor volume was measured with a caliper and was calculated as follows: tumor volume = $0.5 \times \text{length} \times \text{width}^2$. On the 12th day, the mice were sacrificed, then the tumor and major organs (hearts, lungs, livers, kidneys and spleens) were washed with PBS and weighed. Moreover, tumor paraffin sections of three groups were stained with H&E staining to observe pathological changes.

Statistical analysis

Data were reported as mean ± standard error of the mean, using the unpaired Student's *t*-test. Values of **p* < 0.05 and ****p* < 0.001 calculated by GraphPad Prism 7 were considered significant and extremely significant, respectively.

Results and discussion

Solubility determination of chrysoerythrin A SDs

The aqueous solubility of CA and its ball milling products was shown in Table 1. It could be seen that there

Table 1 The solubility of pure CA and its mechanical processed products

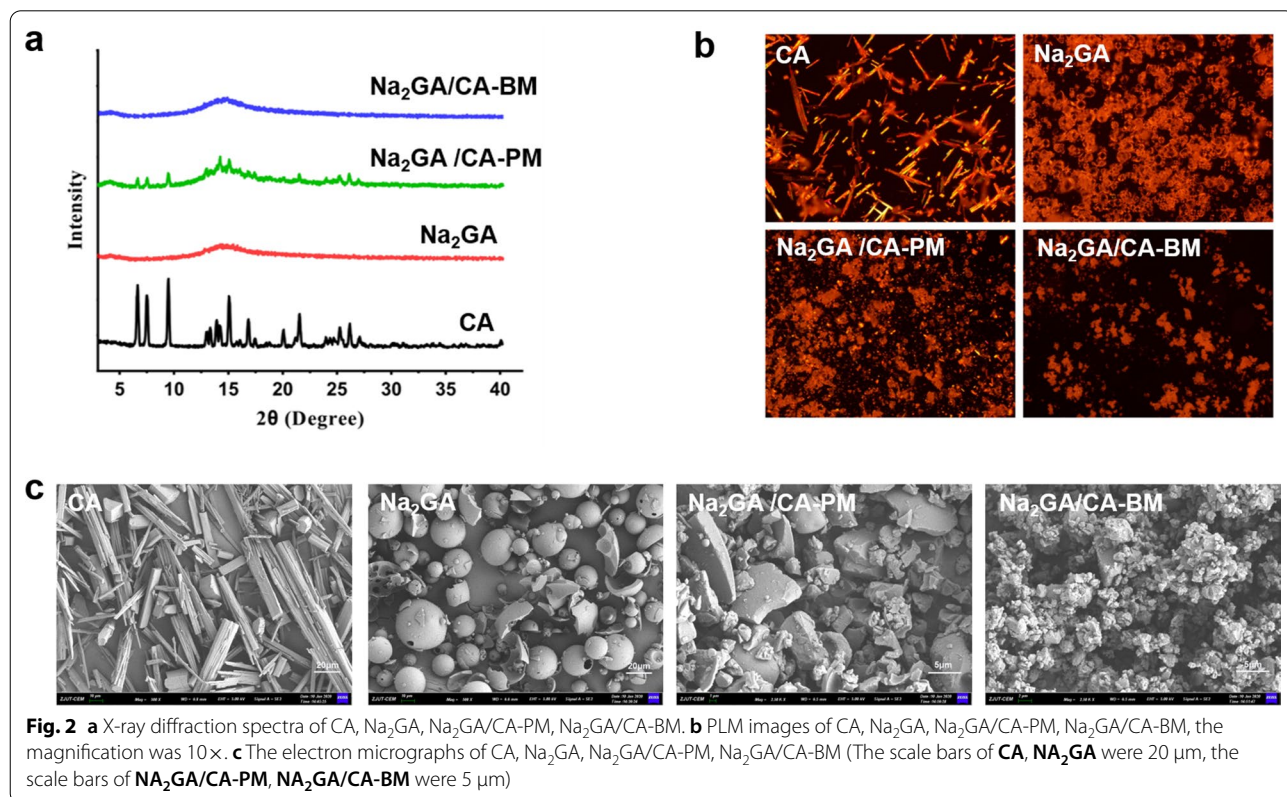
Sample	Ball-milling time (h)	Solubility ($\mu\text{g}/\text{mL}$)	Increase solubility (times)
CA	–	1.68 ± 0.66	–
BM-0.5 h	0.5	38.39 ± 8.86	~23
BM-1.0 h	1	50.97 ± 27.89	~30
BM-1.5 h	1.5	56.21 ± 16.89	~33
BM-2.0 h	2	63.78 ± 11.53	~38
BM-2.5 h	2.5	82.40 ± 25.32	~50
BM-3.0 h	3	65.23 ± 17.16	~39

were significant differences between CA ($1.68 \pm 0.66 \mu\text{g}/\text{mL}$) and the SD samples. In addition, the solubility of CA SDs was gradually increased by prolonging the ball milling time from 0.5 to 2.5 h. The drug milled for long time provided better wettability and dispersibility which was formed as the amorphous complex and encapsulated in a hydrophilic carrier. The solubility of $\text{Na}_2\text{GA}/\text{CA}$ SD was excellently raised after the formation. However, an unwanted decreased of the solubility could be observed after milling for 3 h. It was supposed that further aggregation of the particles resulted in their higher

surface energy with increased time of milling process, and thereby decreasing the solubility [31]. Since the sample created by ball milling for 2.5 h had the best solubility ($82.41 \pm 25.32 \mu\text{g}/\text{mL}$) which was increased about 50 times compared with unprocessed pure CA, it was chose as chrysomycin A SDs candidate to study the subsequent experiments and was described as $\text{Na}_2\text{GA}/\text{CA-BM}$.

Physicochemical changes of chrysomycin A SDs

Physicochemical changes were analyzed by XRD, PLM and SEM. The X-ray diffractograms of CA, Na_2GA , $\text{Na}_2\text{GA}/\text{CA}$ -Pand $\text{Na}_2\text{GA}/\text{CA-BM}$ were shown in Fig. 2a. CA displayed several sharp peaks at diffraction angles (2θ) of 6.67, 7.50, 9.47, 15.09, 21.60, indicating its crystalline form. On the other hand, the characteristic peaks of CA existed in the mechanical treated sample indicating it was still a crystal form. However, the crystallization peaks of CA were markedly decreased in the diffraction spectrum of $\text{Na}_2\text{GA}/\text{CA-PM}$, and even no characteristic peaks were observed in the sample of $\text{Na}_2\text{GA}/\text{CA-BM}$. The phenomenon could be attributed to the completely loss of crystalline of CA owing to high-intensity ball milling process. These XRD results further confirmed that CA which was dispersed in excipient Na_2GA to form an amorphous complex by ball milling.



The micrographs of CA, Na₂GA, Na₂GA/CA-PM and Na₂GA/CA-BM obtained from polarized light microscopy are shown in Fig. 2b. As observed in the unprocessed CA, there was extensive birefringence, confirming its crystalline nature. In the Na₂GA/CA-PM micrograph of the physical mixture, the birefringence of CA was dispersed partially. After mechanochemical treatment, Na₂GA/CA-BM was shown no birefringence which identified the amorphous nature of CA embedded in Na₂GA.

Furthermore, the electron micrographs of CA, Na₂GA, Na₂GA/CA-PM and Na₂GA/CA-BM are shown in Fig. 2c. It could be clearly seen that pure CA was elongated solid and the Na₂GA was composed of hollow spherical particle with a smooth surface texture. On the contrary, the intact morphology of CA and Na₂GA were disappeared and showed a fine and irregularly shaped particle for the ball-milling product Na₂GA/CA-BM, suggesting the amorphous solid phase structure of Na₂GA/CA-BM. The most noteworthy, that the noted particles dispersed more uniformly after being ground for 2.5 h, possibly increased its surface thus improving the velocity of dissolution.

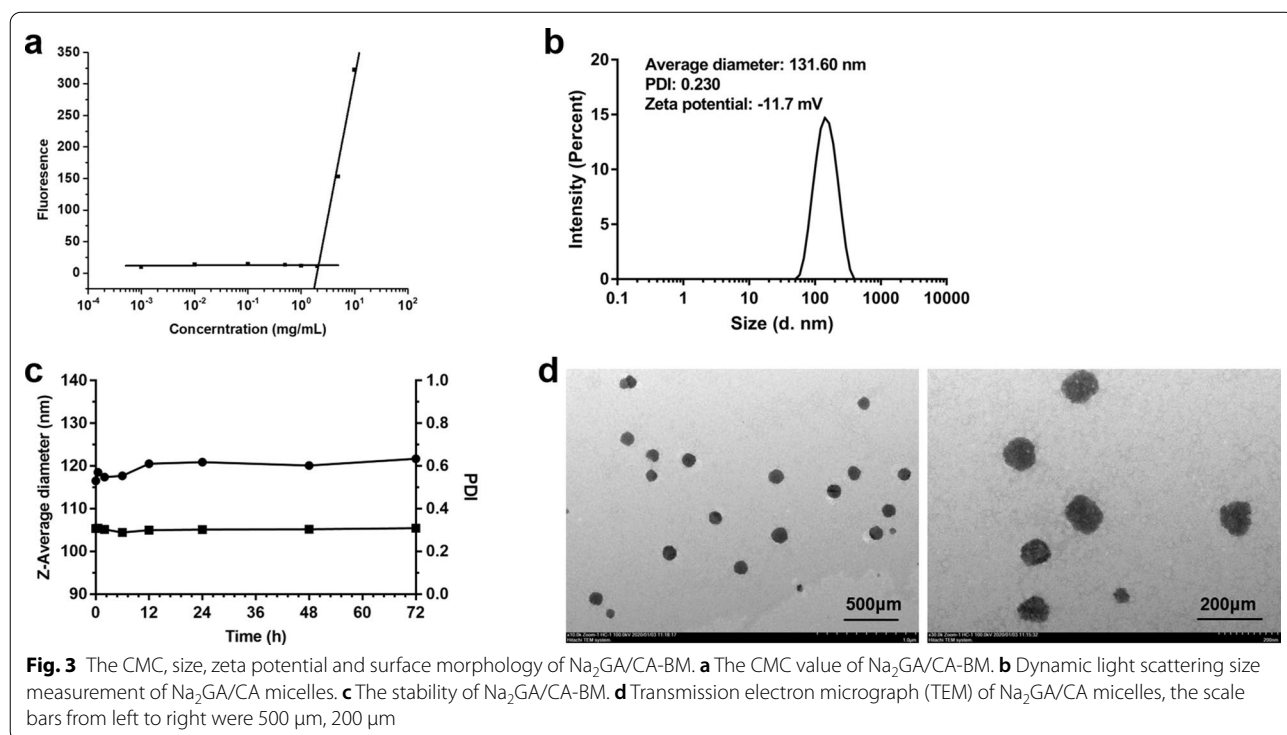
Properties of chrysomycin A micelles in water solution

When the Na₂GA/CA-BM dissolved in water, Na₂GA coated CA to form CA micelles. The critical micelle concentration of Na₂GA/CA-BM was about 1.77 mg/mL (Fig. 3a). The size, zeta potential and surface morphology

of micelles are all crucial for interactions between the cell membranes and micelles. As shown in Fig. 3b, the average diameter of the particle was about 131.6 nm with a narrow size distribution at 25 °C, and its polymer dispersity index (PDI) value was about 0.230. Moreover, the particle has a negative zeta potential which was - 11.7 mV. It was reported that suitable range of particle sizes for evading filtration in reticuloendothelial system (RES) organs was between 100 and 200 nm [32–35]. In addition, the neutral surface charge of particles (zeta potential ± 10 mV) was proved to prolonged blood circulation and facilitate its accumulation at the tumor tissue [33]. Therefore, Na₂GA/CA-BM formed a great candidate to further use in the animal studies due to proper diameter and potential. The particle size showed relatively stable over a span of 72 h incubation in cell culture medium with 10% FBS and a slight increase of size from 116 to 121 nm during the period. The PDI remained relatively the same at about 0.30. Furthermore, the images of micelle appearance observed by TEM are depicted in Fig. 3d. The nano-micelle was spherical with smooth boundaries. The diameter of nano-micelle was about 100 nm and slightly smaller than DLS data because of its shrinkage when dried before TEM detection.

In vitro cytotoxicity and cell uptake

As shown in Fig. 4a, compared with the suspension of free CA, Na₂GA/CA-BM have the significant



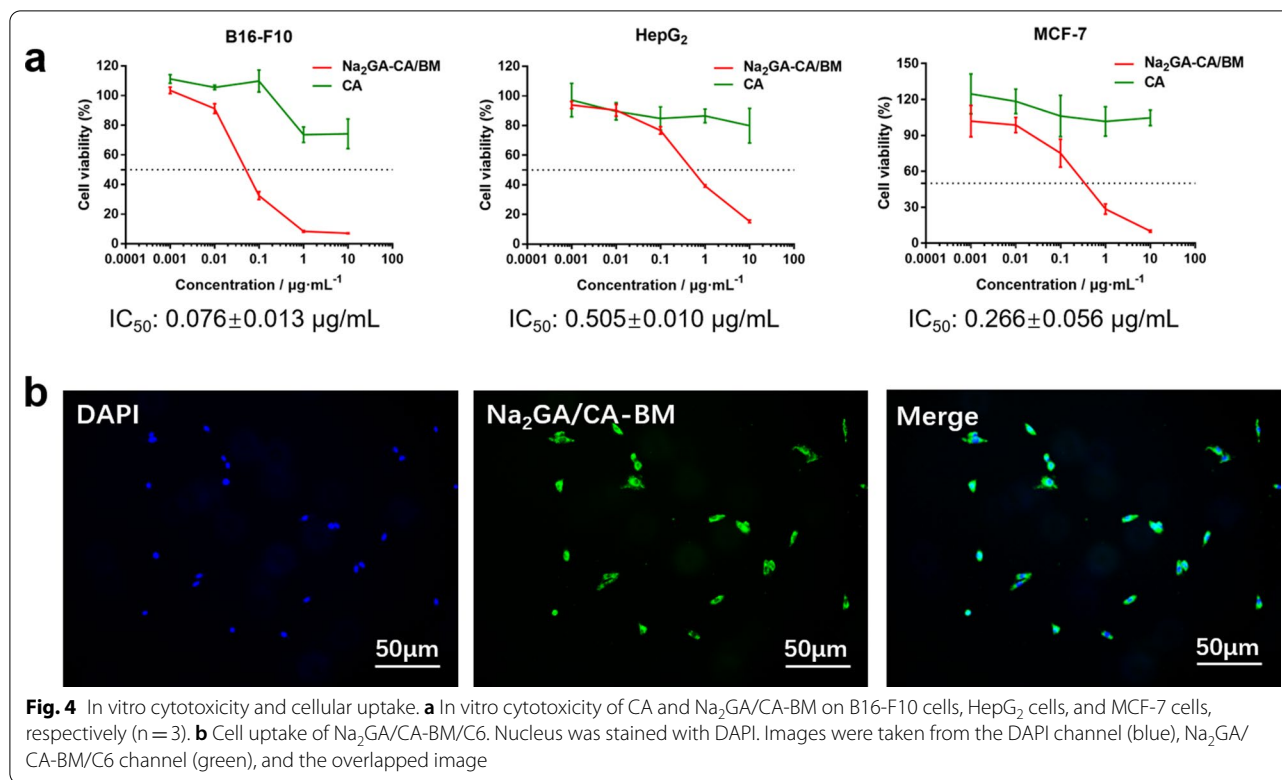


Table 2 Cytotoxicity of Na₂GA in B16-F10, MCF-7 and HepG₂ cell lines

Concentration of Na ₂ GA (µg/mL)	Viability (%)		
	B16-F10	MCF-7	HepG ₂
0.099	97.1 ± 9.5	100.9 ± 7.6	100.9 ± 5.2
0.99	98.0 ± 7.7	108.6 ± 12.7	105.2 ± 2.9
9.9	92.9 ± 4.4	104.2 ± 9.3	102.1 ± 2.4
99	95.1 ± 3.6	97.0 ± 19.2	98.1 ± 1.5
990	72.0 ± 6.9	73.1 ± 4.3	90.6 ± 5.3

inhibition ability in all three kinds of tumor cells. The half maximal inhibitory concentrations (IC₅₀) of Na₂GA/CA-BM were 0.076 ± 0.013 µg/mL on B16-F10 cells, 0.505 ± 0.010 µg/mL on HepG₂ cells, and 0.266 ± 0.056 µg/mL on MCF-7 cells, respectively. Especially, the cytotoxicity of Na₂GA/CA-BM on B16-F10 cells was statistically significant compared with other two tumor cell lines. As shown in Table 2, the survival rate of all three cell lines was between 72 and 108.6%, which indicated that Na₂GA itself possessed almost no cytotoxicity in all tested cell lines in the concentration range of 0.099–990 µg/mL. Therefore, Na₂GA/CA-BM enhanced the cytotoxic ability of CA, and all obtained cytotoxic action of Na₂GA/CA-BM

was due to the CA effect. Mechanical ball milling and Na₂GA increased the solubility of CA in water, resulting in the increase of its concentration in suspension.

As for the colocalization and internalization by B16-F10 cells of coumarin-6-loaded Na₂GA/CA-BM (Na₂GA/CA-BM/C6), the fluorescence images were shown in Fig. 4b, indicating that Na₂GA/CA-BM/C6 was quickly taken up by B16-F10 cells and located in cytoplasm of the tumor cells.

Pharmacokinetic evaluation

The concentration–time curves of CA in mice plasma are depicted in Fig. 5a, and the pharmacokinetic parameters are summarized in Table 3. From the figure, it could be clearly seen that the bioavailability of Na₂GA/CA-BM was improved than pure CA. After intragastric administration, CA and Na₂GA/CA-BM both distributed rapidly and reached the max blood concentration at 0.5 h. What’s more, the accumulation time in the body of Na₂GA/CA-BM was longer about twofold than the retention time of free CA. Then, the free CA was cleared faster from blood than Na₂GA/CA-BM, so Na₂GA/CA-BM had a better blood circulation in the body. Compared with CA, the area under the curve of Na₂GA/CA-BM was increased about 1.8 times larger, and the plasma clearance was dramatically decreased.

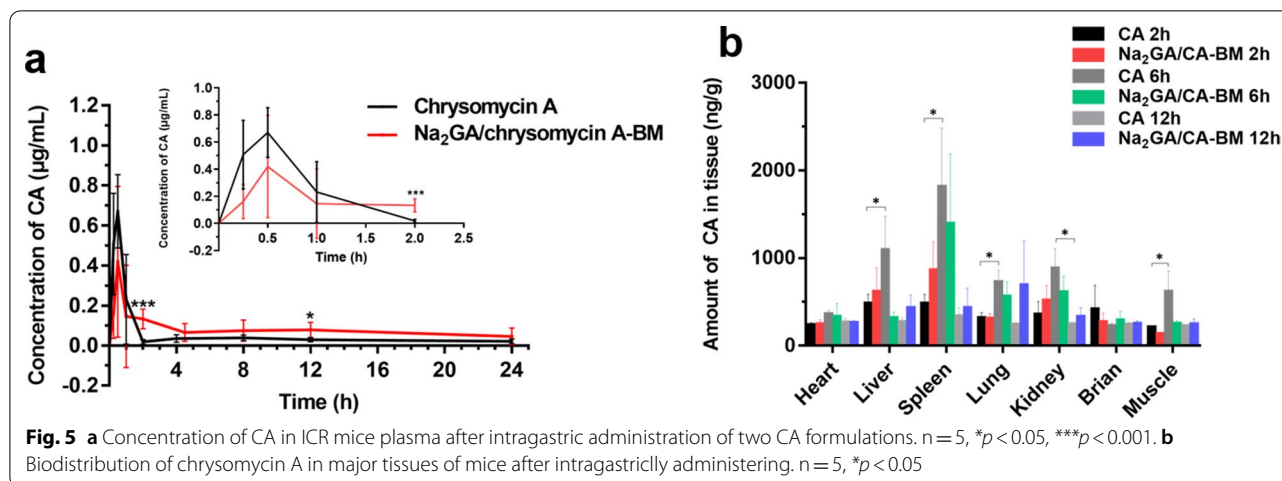


Table 3 The pharmacokinetic parameters of pure chrysomycin A and Na₂GA/CA-BM

Samples	C _{max} (µg/mL)	T _{max} (h)	T _{1/2} (h)	AUC _{0→t} (µg/mL·h)	AUC _{0→∞} (µg/mL·h)	CL (L/h/kg)
CA	0.67	0.50	7.55	1.62	1.72	29.02
Na ₂ GA/CA-BM	0.42	0.50	13.98	2.17	3.09	17.14

C_{max} peak plasm concentration, T_{max} time to reach peak concentration, T_{1/2} half life, AUC area under the plasm concentration–time curve, CL plasm clearance

Tissue distribution study

Figure 5b depicts the distribution concentration of CA in major tissues of mice including heart, liver, spleen, lung, kidney, brain, skeletal muscle after oral dose of 50 mg/kg of either Na₂GA/CA-BM or CA. After intragastric administration for 2 h, the concentration of CA (Na₂GA/CA-BM group) was high in spleen, and reached to the highest blood concentration at 6 h, after that CA gradually cleared and finally expelled at about 12 h. As for free CA group, CA was distributed mainly in spleen, liver, lung, kidney and muscle, and slowly cleared after 12 h. The main metabolic organ of CA was liver and spleen, while Na₂GA/CA-BM was metabolized mainly in spleen after 6 h. Generally, large size of particles were preferentially absorbed by the liver, and small particles were easily cleared by the spleen, which led to the change in metabolic site of drug [36, 37]. In comparison, Na₂GA/CA-BM showed longer blood accumulation in body than free CA after 12 h, which was consistent with the results of the pharmacokinetic study.

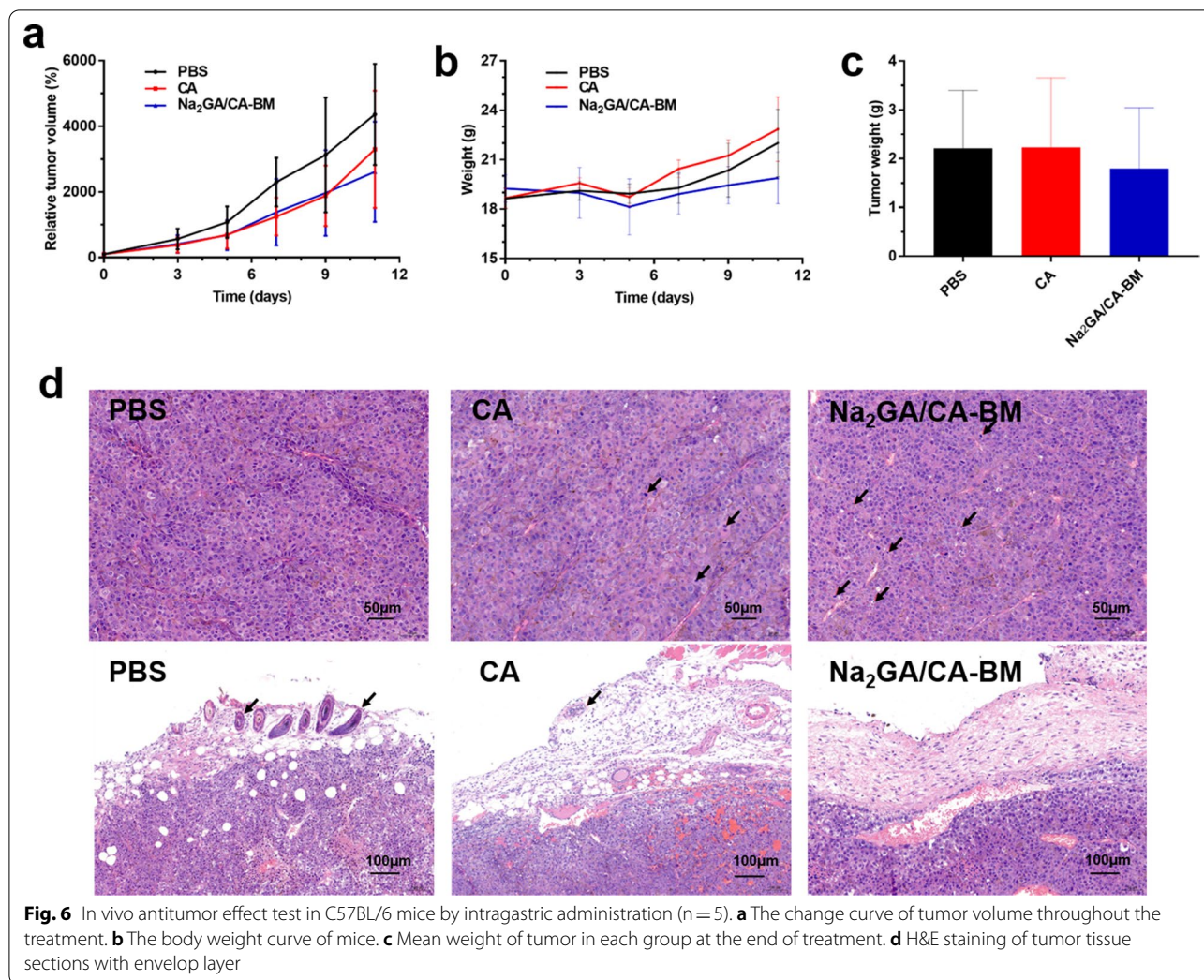
In vivo antitumor efficacy

Due to the better performance on the solubility and bioavailability, we next evaluated the antitumor ability of Na₂GA/CA-BM on B16-F10 tumor-bearing C57BL/6 mice. As shown in Fig. 6a, CA and Na₂GA/CA-BM both inhibited the growth of B16-F10 tumors compared with

the control group. Meanwhile, Na₂GA/CA-BM showed better tumor suppression ability throughout the treatment, and the tumor inhibition rate was closed 28.76%. From Fig. 6b, it was found that none of the mice loss body weight obviously after treating CA formulations, which indicated no potential systemic toxicities of CA and Na₂GA/CA-BM.

After tumors excision, the weights (Fig. 6c) of tumors treated with Na₂GA/CA-BM (1.800 ± 1.246 g) were lower than those of the mice treated with CA (2.230 ± 1.429 g) or PBS (2.212 ± 1.192 g). In addition, the tumor weights of CA group showed no significant differences compared with the control group.

H&E staining were shown to observe pathological changes of tumor cells in three groups, As shown in Fig. 6d, the tumor cells were dense and had abundant vascular tissue in all three groups. Karyopycnosis and deep staining could be seen, which meant apoptosis and necrosis of cancer cells. Thus, different degrees of apoptosis were seen in tumors treated with CA and Na₂GA/CA-BM. In comparison, a large amount of excessive vacuolization and more apoptosis cells were observed in the tissue section of Na₂GA/CA-BM group. Moreover, various size tumor cells could be seen in the envelop layer of tumor tissue treated with PBS and the free CA, rather than in tumor layer of Na₂GA/CA-BM group, indicating the excellent antitumor ability of Na₂GA/CA-BM.



Conclusions

In the present study, an amorphous CA solid dispersion was successfully prepared by mechanical ball milling. As compared to the free CA, Na₂GA/CA-BM exhibited superior solubility evidenced by a about 50-fold increase. The physicochemical characteristics analysis showed that CA was dispersed uniformly in the hydrophilic carrier (Na₂GA) and transformed from crystals into amorphous state by ball milling. When Na₂GA/CA-BM dissolved in water, CA encapsulated by Na₂GA was self-formed to micelles. Consistent with the amorphous nature and self-formed micelles of Na₂GA/CA-BM, it showed significant improvement of pharmacokinetic behavior in mice, which increased 1.8 times in oral bioavailability. Moreover, Na₂GA/CA-BM also exhibited a stronger antitumor ability than CA due to the improvement of oral bioavailability. In summary, our work illustrated an unprecedented and

environment-friendly preparation of the CA formulation by ball milling approach, which are promising to enhance the oral bioavailability and antitumor ability of CA, might be considered for efficient anticancer therapy.

Acknowledgements

This work was supported by Grants from the National Key R&D Program of China (2018YFC0311005), the National Natural Science Foundation of China (No. 22075247), and the Zhejiang Provincial Natural Science Foundation of China (No. LGF21C100001), Research Foundation for Advanced Talents of Beijing Technology and Business University (No. 19008020158).

Authors' contributions

XS, HZ and HW conceived and designed the experiments. FS provided chrysoerythrin A. ZX, YC, SZ, XG and YH performed experiments. QZ and JX provided technical support for the preparation of Na₂GA/CA-BM, DX provided technical support for the antitumor activity. ZX analyzed data and wrote the article. XS interpreted data and reviewed the manuscript. All authors read and approved the final manuscript.

Availability of data and materials

The datasets used and/or analysed during the current study are available from the corresponding author on reasonable request.

Declarations

Ethics approval and consent to participate

All experimental procedures involving animals performed in this study were previously approved and certified (No. 20200824109) by the animal experiment center of Zhejiang University of Technology, which performed in strict compliance with the PR China legislation for the use and care of laboratory animals.

Consent for publication

Not applicable.

Competing interests

The authors declare that they have no competing interests.

Author details

¹Collaborative Innovation Center of Yangtze River Delta Region Green Pharmaceuticals and College of Pharmaceutical Science, Zhejiang University of Technology, Hangzhou 310014, China. ²School of Light Industry, Beijing Technology and Business University, Beijing 100048, China.

Received: 28 February 2021 Accepted: 25 May 2021

Published online: 31 May 2021

References

- Matson JA, Rose WC, Bush JA, Myllymaki R, Bradner WT, Doyle TW. Antitumor activity of chrysomycins M and V. *J Antibiot*. 1989;42:1446–8.
- Weiss U, Yoshihira K, Highet RJ, White RJ, Wei TT. The chemistry of the antibiotics chrysomycin A and B Antitumor activity of chrysomycin A. *J Antibiot*. 1982;35:1194–201.
- Li Y, Huang X, Ishida K, Maier A, Kelter G, Jiang Y, Peschel G, Menzel K, Li M, Wen M, Xu L, Grabley S, Fiebig H, Jiang C, Hertweck C, Sattler I. Plasticity in gilvocarcin-type C-glycoside pathways: discovery and antitumoral evaluation of polycarcin V from *Streptomyces polyformus*. *Org Biomol Chem*. 2008;6:3601–5.
- Wada S, Sawa R, Iwanami F, Nagayoshi M, Kubota Y, Iijima K, Hayashi C, Shibuya Y, Hatano M, Igarashi M, Kawada M. Structures and biological activities of novel 4'-acetylated analogs of chrysomycins A and B. *J Antibiot*. 2017;70:1150.
- Kudinova MK, Kuliaeva VV, Potapova NP, Rubasheva LM, Maksimova TS. Separation and characteristics of the components of the antibiotic virenomycin. *Antibiotiki*. 1982;27:507–11.
- Muralikrishnan B, Dan VM, Vinodh JS, Jamsheena V, Ramachandran R, Thomas S, Dastager SG, Kumar KS, Lankalapalli RS, Kumar RA. Antimicrobial activity of chrysomycin A produced by *Streptomyces* sp. against *Mycobacterium tuberculosis*. *Rsc Adv*. 2017;7:36335–9.
- Jain SK, Pathania AS, Parshad R, Raina C, Ali A, Gupta AP, Kushwaha M, Aravinda S, Bhushan S, Bharate SB, Vishwakarma RA. Chrysomycins A-C, antileukemic naphthocoumarins from *Streptomyces sporoverrucosus*. *Rsc Adv*. 2013;3:21046–53.
- Lorico A, Long BH. Biochemical characterisation of elsamicin and other coumarin-related antitumour agents as potent inhibitors of human topoisomerase II. *Eur J Cancer*. 1993;29A:1985–91.
- Gu Q, Xing JZ, Huang M, He C, Chen J. SN-38 loaded polymeric micelles to enhance cancer therapy. *Nanotechnology*. 2012. <https://doi.org/10.1088/0957-4484/23/20/205101>.
- Liu Y, Yang G, Baby T, Tengjisi, Chen D, Weitz DA, Zhao C. Stable polymer nanoparticles with exceptionally high drug loading by sequential nanoprecipitation. *Angew Chem Int Edit*. 2020;59:4720–8.
- Hammoud Z, Khreich N, Auezova L, Fourmentin S, Elaissari A, Greige-Gerges H. Cyclodextrin-membrane interaction in drug delivery and membrane structure maintenance. *Int J Pharmaceut*. 2019;564:59–76.
- Terauchi M, Inada T, Tonegawa A, Tamura A, Yamaguchi S, Harada K, Yui N. Supramolecular inclusion complexation of simvastatin with methylated beta-cyclodextrins for promoting osteogenic differentiation. *Int J Biol Macromol*. 2016;93:1492–8.
- Javeer SD, Patole R, Amin P. Enhanced solubility and dissolution of simvastatin by HPMC-based solid dispersions prepared by hot melt extrusion and spray-drying method. *J Pharm Investig*. 2013;43:471–80.
- Wang F, Xiao X, Yuan Y, Liu J, Liu Y, Yi X. Solubilization of phloretin via steviol glycoside-based solid dispersion and micelles. *Food Chem*. 2020. <https://doi.org/10.1016/j.foodchem.2019.125569>.
- Saggar S, Upadhyay A, Goswami M. Formulation and evaluation of solid self-emulsifying drug delivery system of bambuterol hydrochloride. *Indian J Pharm Sci*. 2019;81:661–72.
- Zhang Q, Polyakov NE, Chistyachenko YS, Khvostov MV, Frolova TS, Tolstikova TG, Dushkin AV, Su W. Preparation of curcumin self-micelle solid dispersion with enhanced bioavailability and cytotoxic activity by mechanochemistry. *Drug Deliv*. 2018;25:198–209.
- Bahri M, Kazemian H, Rohani S, Haghghat F. Mechanochemical synthesis of CPM-5: a green method. *Chem Eng Technol*. 2017;40:88–93.
- Wei G, Li Y, Zhang L, Cai S, Zhu T, Li Z, Mo J. Synthesis of bentonite-supported Fe(II) and heteropolyacid (HPW) composite through a mechanochemical processing. *Appl Clay Sci*. 2018;152:342–51.
- Da Silva CCP, de Melo CC, Souza MS, Diniz LF, Carneiro RL, Ellena J. 5-Fluorocytosine/5-fluorouracil drug-drug cocrystal: a new development route based on mechanochemical synthesis. *J Pharm Innov*. 2019;14:50–6.
- Douroumis D, Ross SA, Nokhodchi A. Advanced methodologies for cocrystal synthesis. *Adv Drug Deliver Rev*. 2017;117:178–95.
- Xu W, Wen M, Yu J, Zhang Q, Polyakov NE, Dushkin AV, Su W. Mechanochemical preparation of kaempferol intermolecular complexes for enhancing the solubility and bioavailability. *Drug Dev Ind Pharm*. 2018;44:1924–32.
- Sun X, Zhu D, Cai Y, Shi G, Gao M, Zheng M. One-step mechanochemical preparation and prominent antitumor activity of SN-38 self-micelle solid dispersion. *Int J Nanomed*. 2019;14:2115–26.
- Boldyrev VV. Mechanochemical modification and synthesis of drugs. *J Mater Sci*. 2004;39:5117–20.
- Descamps M, Willart JF. Perspectives on the amorphisation/milling relationship in pharmaceutical materials. *Adv Drug Deliver Rev*. 2016;100:51–66.
- Pompei R, Laconi S, Ingiani A. Antiviral properties of glycyrrhizic acid and its semisynthetic derivatives. *Mini-Rev Med Chem*. 2009;9:996–1001.
- Bernela M, Ahuja M, Thakur R. Enhancement of anti-inflammatory activity of glycyrrhizic acid by encapsulation in chitosan-katira gum nanoparticles. *Eur J Pharm Biopharm*. 2016;105:141–7.
- Su X, Wu L, Hu M, Dong W, Xu M, Zhang P. Glycyrrhizic acid: a promising carrier material for anticancer therapy. *Biomed Pharmacother*. 2017;95:670–8.
- Yang F, Zhang Q, Liang Q, Wang S, Zhao B, Wang Y, Cai Y, Li G. Bioavailability enhancement of paclitaxel via a novel oral drug delivery system: paclitaxel-loaded glycyrrhizic acid micelles. *Molecules*. 2015;20:4337–56.
- Kong R, Zhu X, Meteleva ES, Chistyachenko YS, Sunstova LP, Polyakov NE, Khvostov MV, Baev DS, Tolstikova TG, Yu J, Dushkin AV, Su W. Enhanced solubility and bioavailability of simvastatin by mechanochemically obtained complexes. *Int J Pharmaceut*. 2017;534:108–18.
- Selyutina OY, Polyakov NE, Korneev DV, Zaitsev BN. Influence of glycyrrhizin on permeability and elasticity of cell membrane: Perspectives for drugs delivery. *Drug Deliv*. 2016;23:858–65.
- Du L, Dushkin AV, Chistyachenko YS, Polyakov NE, Su W. Investigation the inclusion complexes of valsartan with polysaccharide arabinogalactan from larch *Larix sibirica* and (2-hydroxypropyl)-beta-cyclodextrin: preparation, characterization and physicochemical properties. *J Incl Phenom Macro*. 2016;85:93–104.
- Chen M, Li W, Zhang X, Dong Y, Hua Y, Zhang H, Gao J, Zhao L, Li Y, Zheng A. In vitro and in vivo evaluation of SN-38 nanocrystals with different particle sizes. *Int J Nanomedicine*. 2017;12:5487–500.
- Li S, Huang L. Pharmacokinetics and biodistribution of nanoparticles. *Mol Pharmaceut*. 2008;5:496–504.
- Sun Q, Zhou Z, Qiu N, Shen Y. Rational design of cancer nanomedicine: nanoproperty integration and synchronization. *Adv Mater*. 2017. <https://doi.org/10.1002/adma.201606628>.

35. Liu D, Mori A, Huang L. Role of liposome size and RES blockade in controlling biodistribution and tumor uptake of GM1-containing liposomes. *Biochim Biophys Acta*. 1992;1104:95–101.
36. Li M, Al-Jamal KT, Kostarelos K, Reineke J. Physiologically based pharmacokinetic modeling of nanoparticles. *ACS Nano*. 2010;4:6303–17.
37. Hoshyar N, Gray S, Han H, Bao G. The effect of nanoparticle size on in vivo pharmacokinetics and cellular interaction. *Nanomedicine*. 2016;11:673–92.

Publisher's Note

Springer Nature remains neutral with regard to jurisdictional claims in published maps and institutional affiliations.

Ready to submit your research? Choose BMC and benefit from:

- fast, convenient online submission
- thorough peer review by experienced researchers in your field
- rapid publication on acceptance
- support for research data, including large and complex data types
- gold Open Access which fosters wider collaboration and increased citations
- maximum visibility for your research: over 100M website views per year

At BMC, research is always in progress.

Learn more biomedcentral.com/submissions

